

Andreev reflection and Kondo effect in tunnelling through a superconducting grain

This article has been downloaded from IOPscience. Please scroll down to see the full text article.

2001 J. Phys.: Condens. Matter 13 7371

(<http://iopscience.iop.org/0953-8984/13/33/317>)

View [the table of contents for this issue](#), or go to the [journal homepage](#) for more

Download details:

IP Address: 171.66.16.238

The article was downloaded on 17/05/2010 at 04:32

Please note that [terms and conditions apply](#).

Andreev reflection and Kondo effect in tunnelling through a superconducting grain

Shi-Jie Xiong¹ and Yeong-Der Yao²

¹ National Laboratory of Solid State Microstructures and Department of Physics, Nanjing University, Nanjing 210093, China

² Institute of Physics, Academia Sinica, Taipei, Taiwan

Received 23 May 2001

Published 2 August 2001

Online at stacks.iop.org/JPhysCM/13/7371

Abstract

We investigate tunnelling of electrons through a superconducting grain at nanometre scales. The conductance is computed from a network of many-body states, taking into account contributions from normal tunnelling and Andreev reflection. The contribution from Andreev reflection is maximized if the grain ground state is degenerate with a state having an extra pair of electrons. By increasing the Coulomb interaction within the grain, the system exhibits a crossover from the Andreev behaviour to the Kondo behaviour at a point where the charging energy is equal to the pairing energy.

1. Introduction

In recent years there has been continuous interest in investigations of properties of small superconducting grains [1–5]. The finite size of the grain leads to splitting of energy levels and the Coulomb blockade effect. The even–odd parity of occupation number induced by Coulomb blockade has been observed in experiments [1]. In measurements of the I – V curves of tunnelling through nanometer-sized Al grains, Ralph, Black and Tinkham [2] have shown that a gap significantly larger than the typical level spacing between single-electron eigenstates still exists. However, if the grain size is further reduced (<5 nm), no gap in the spectrum can be detected.

The tunnelling conductance through a superconducting grain in the Coulomb blockade regime has been investigated by several authors [3]. In these studies the ordinal order parameter from the mean-field theory is used for the grain. As pointed out by Jankó *et al* [4], the use of the order parameter in a system with a fixed number of electrons is problematical because the superconducting order is off-diagonal in particle number. This problem is caused by the level splitting and the Coulomb blockade as in a grain at nanometer scales the charging energy plus the level spacing is comparable with the pairing energy [1, 2]. Several theoretical approaches have been developed to address the crossover between the superconducting and normal state at nanometer scales beyond the concept of the mean-field

gap [5–7]. Since the zero resistance and the Meissner effect disappear when the size shrinks to a few nanometers, an appropriate quantity is needed to illustrate the remnant effects of superconductivity. The parity gap Δ_M , which is related to the extra ground-state energy of a system with an unpaired electron and can be determined in the canonical ensemble, was proposed in [6].

Because the characteristic features of bulk superconductors are no longer retained in a grain in the presence of Coulomb interaction, it is interesting to investigate the tunnelling process in a theoretical approach which does not rely on the mean-field order parameter off-diagonal in electron number. In this paper we calculate the tunnelling conduction in various values of Coulomb interaction, gate voltage and temperature. We solve the grain Hamiltonian exactly by using the method of [8]. Then an equivalent multichannel network of many-body states [9] which represents the Schrödinger equations of the system is constructed to describe the tunnelling processes. The results show that the contribution from Andreev reflection is maximized if the ground state of the grain is degenerate with the state having an extra pair of electrons. By increasing the Coulomb interaction the Andreev reflection is suppressed and the system shows the characteristics of normal quantum dots. Especially, if the Coulomb energy is larger than the pairing energy, the Kondo effect can be observed. We illustrate the crossover from the Andreev behaviour to the Kondo behaviour in increasing the Coulomb energy.

The paper is organized as follows: in the next section we describe the Hamiltonian of the system and the basic formulas; in the third section the numerical results and their physical meanings are presented; in the last section a brief summary is given.

2. Hamiltonian and basic formulas

We consider a superconducting grain embedded between two leads:

$$H = H_{SC} + H_L + H_C \quad (1)$$

where H_{SC} is the sub-Hamiltonian of the grain,

$$H_{SC} = \sum_{j\sigma} (\epsilon_j^0 + V_g) c_{j\sigma}^\dagger c_{j\sigma} - \lambda d \sum_{ij} c_{i+}^\dagger c_{i-}^\dagger c_{j-} c_{j+} + (en)^2 / (2C) \quad (2)$$

H_L stands for the one-dimensional leads,

$$H_L = \sum_{\langle mm' \rangle (\neq 0)\sigma} t_0 a_{m\sigma}^\dagger a_{m'\sigma} + \sum_{m(\neq 0),\sigma} \epsilon_0 a_{m\sigma}^\dagger a_{m\sigma} \quad (3)$$

and H_C is the coupling between them,

$$H_C = \sum_{j\sigma} \left(t a_{-1,\sigma}^\dagger c_{j,\sigma} + t a_{1,\sigma}^\dagger c_{j,\sigma} + \text{h.c.} \right). \quad (4)$$

Here, $c_{j\sigma}^\dagger$ and $a_{m\sigma}^\dagger$ create an electron of spin σ in the j th level of grain and on the m th site of leads, respectively, $n = \sum_{j\sigma} c_{j\sigma}^\dagger c_{j\sigma}$, C is the grain capacitance and λ is the strength of pairing interaction. We assume equidistant levels ϵ_j^0 with spacing d . The position of the grain is at $m = 0$. The states on the grain are coupled with the leads by hopping t . The gate voltage V_g is used to tune the particle number. As H_{SC} is a BCS reduced Hamiltonian, only N levels within the range of Debye frequency are taken into account. In the leads the site energy is ϵ_0 and the nearest-neighbour hopping is t_0 .

H_{SC} can be exactly diagonalized [8]. Since the interaction terms in H_{SC} only scatter the pair from one level to another, the labels of the singly occupied levels and their spins are good quantum numbers. For an isolated grain the particle number M is also a good quantum number. The lowest-lying eigenstate with n_d doubly occupied levels and a set of n_s singly occupied levels with specified spins, (S, Σ) , is [8]

$$\Psi(M, S, \Sigma) = \frac{1}{R} \prod_{l=1}^{n_d} \left(\sum_{j \notin S} \frac{c_{j+}^\dagger c_{j-}^\dagger}{2\epsilon_j^0 - e_l} \right) \prod_{(i,\sigma) \in (S,\Sigma)} c_{i\sigma}^\dagger |0\rangle \quad (5)$$

with R the normalization factor, $M = 2n_d + n_s$ and e_l the particular solutions of equations [8]

$$\frac{1}{\lambda d} + \sum_{l'=1(\neq l)}^{n_d} \frac{2}{e_{l'} - e_l} = \sum_{j \notin S} \frac{1}{2\epsilon_j^0 - e_l}. \quad (6)$$

The eigenenergy of this state is $\mathcal{E}(M, S) = \mathcal{E}_0(M, S) + MV_g + \frac{(eM)^2}{2C}$ with $\mathcal{E}_0(M, S) = \sum_{l=1}^{n_d} e_l + \sum_{j \in S} \epsilon_j^0$. For given Fermi level E_F , at zero temperature the particle number M is determined by inequalities

$$\begin{aligned} \min_S [\mathcal{E}(M+1, S)] &\geq \min_S [\mathcal{E}(M, S)] + E_F \\ \min_S [\mathcal{E}(M-1, S)] + E_F &\geq \min_S [\mathcal{E}(M, S)]. \end{aligned} \quad (7)$$

Note that states described by equation (5) have a fixed number of electrons on the grain, while the mean-field superconducting states are expressed in the grand canonical ensemble. Thus, they are suitable for taking into account the restriction in the electron number on the grain due to the Coulomb blockade. In calculating the tunnelling conductance, we consider the following states containing the grain states plus one tunnelling electron or hole [9]:

$$\begin{aligned} \Phi(M, S, \Sigma, m, \sigma) &= a_{m\sigma}^\dagger \Psi(M, S, \Sigma) |F\rangle \\ \Phi(M+2, S, \Sigma, \bar{m}, \sigma) &= a_{m\sigma} \Psi(M+2, S, \Sigma) |F\rangle \\ \Phi(M+1, S, \Sigma) &= \Psi(M+1, S, \Sigma) |F\rangle \\ \Phi(M-1, S, \Sigma, -1, \sigma, 1, \sigma') &= a_{-1\sigma}^\dagger a_{1\sigma'}^\dagger \Psi(M-1, S, \Sigma) |F\rangle \\ \Phi(M+1, S, \Sigma, -\bar{1}, \sigma, \bar{1}, \sigma') &= a_{-1\sigma} a_{1\sigma'} \Psi(M+1, S, \Sigma) |F\rangle \end{aligned} \quad (8)$$

where $|F\rangle$ denotes the Fermi sea in the leads. The last two states in equation (8) contain two electrons or holes in the leads, representing the lowest order of the cotunnelling process. An eigenfunction can be expressed as a linear combination of them

$$\begin{aligned} \sum_{i(\pm 1), m(\neq 0)} \sum_{S, \Sigma, \sigma} p_i(m, \sigma, S, \Sigma) \Phi(M-i+1, S, \Sigma, m, \sigma) &+ \sum_{S, \Sigma} q(S, \Sigma) \Phi(M+1, S, \Sigma) \\ &+ \sum_{S, \Sigma} c_1(S, \Sigma) \Phi(M-1, S, \Sigma, -1, \sigma, 1, \sigma') \\ &+ \sum_{S, \Sigma} c_{-1}(S, \Sigma) \Phi(M+1, S, \Sigma, -\bar{1}, \sigma, \bar{1}, \sigma'). \end{aligned} \quad (9)$$

If M is even, for given σ one has equations

$$\chi_i p_i(m) + \text{sign}(i) t_0 [p_i(m+1) + p_i(m-1)] = E p_i(m) \quad \text{for } m \neq 0, 1, -1 \quad (10)$$

$$\chi_i p_i(\pm 1) + \text{sign}(i) t_0 p_i(\pm 2) + t_{i,1} q + t_{i,2} c_i = E p_i(\pm 1) \quad (11)$$

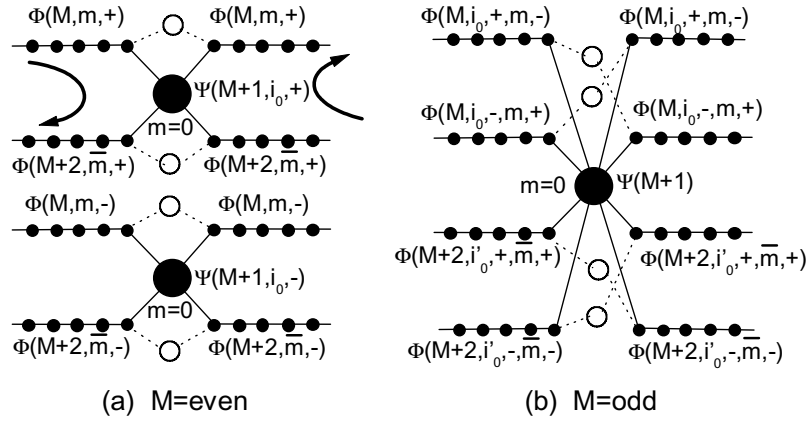


Figure 1. Schematic illustration of the Schrödinger equations of many-body states with a tunnelling electron or hole. The circles represent the coefficients in the linear combination of equation (9); the lines illustrate the couplings between them in the Schrödinger equations. The open circles and the broken lines denote the cotunnelling process. (a) M is even. The Andreev reflection is indicated by thick arrows. (b) M is odd. Spin degrees of freedom are mixed.

where

$$q = \sum_{i(\pm 1), m(\pm 1)} t_{i,1} p_i(m) / (E - \chi_{0,0})$$

$$c_i = \sum_{m(\pm 1)} t_{i,2} p_i(m) / (E - \chi_{0,i})$$

$$\chi_{1,0} = \mathcal{E}(M, 0) + \epsilon_0 \quad \chi_{-1,0} = \mathcal{E}(M+2, 0) - \epsilon_0$$

$$\chi_{0,0} = \mathcal{E}(M+1, S) \quad \chi_{0,i} = \mathcal{E}(M-2i+1, S) + 2 \text{sign}(i)\epsilon_0$$

with S the singly occupied level as close as possible to E_F , and

$$t_{i,1(2)} = \langle \psi_{i,1(2)} | H_C | \Phi(M-i+1, 0, 0, -1, \sigma) \rangle$$

$$\psi_{i,1} = \Phi(M+1, S, \sigma)$$

$$\psi_{i,2} = \Phi(M-2i+1, S, -\sigma, -1, \sigma, \hat{i}, \sigma)$$

with $\hat{i} = 1$ for $i = 1$ and $\hat{i} = \bar{1}$ for $i = -1$. Here, for simplicity we include only the low-lying configuration for S . The equations can be easily extended to include all the intermediate states by replacing terms $t_{i,1}q$ and $t_{i,2}c_i$ in equation (11) with sums over possible configurations. Schrödinger equations (10) and (11) correspond to an equivalent two-channel network as shown in figure 1(a). The upper channel represents the propagation of an electron above the Fermi level of the leads together with M (even) paired electrons on the grain. The lower channel stands for a hole below the Fermi level accompanied by $M+2$ paired electrons on the grain. If one electron above the Fermi level is injected onto the left lead, it may be reflected back to the upper channel as an electron, or to the lower channel as a hole, referred as the Andreev reflection. The injected electron can also be transmitted to the right lead as an electron, representing the normal tunnelling, or as a hole, equivalent to an electron flowing from the right lead to the grain. On the other hand, when a hole is injected from the right lead, it can also be reflected or transmitted as a hole or as an electron. The flow of electrons and holes results in current in opposite directions. Thus, when a bias is applied to enhance the potential of the left lead, the left electron channel and the right hole channel are incoming ones

and the other two are outgoing ones for the current through the network. From the Schrödinger equations listed above, we can solve the 2×2 transmission matrix of the network

$$s_{ii';\sigma\sigma'}(M) = \frac{2ie^{i(k_i+k_{i'})}\sqrt{\sin(k_i)\sin(k_{i'})}u_{ii'}\delta_{\sigma\sigma'}}{2e^{ik_{i'}}v_{ii'} - 1} \quad (12)$$

where i and i' are pseudo-spin indices distinguishing the particle ($i, i' = 1$) and hole ($i, i' = -1$), k_i the corresponding momentum satisfying the dispersion relation $E - \chi_i = 2 \text{sign}(i)t_0 \cos k_i$ and

$$u_{ii'} = -\frac{t_{i,1}t_{i',1}\left(1 - \frac{2e^{ik_{i'}}t_{-i,2}^2\delta_{ii'}}{t_0(E-\chi_{0,-i})}\right)}{2e^{ik_{i'}}\left(t_{-i',1}^2 + t_{-i',2}^2\frac{E-\chi_{0,0}}{E-\chi_{0,-i'}}\right) - t_0(E-\chi_{0,0})} + \frac{t_{i,2}^2\delta_{i,i'}}{t_0(E-\chi_{0,i})} \quad (13)$$

$$v_{ii'} = -\frac{t_{i',1}^2\left(1 - \frac{2e^{ik_{i'}}t_{-i',2}^2}{t_0(E-\chi_{0,-i'})}\right)}{2e^{ik_{i'}}\left(t_{-i',1}^2 + t_{-i',2}^2\frac{E-\chi_{0,0}}{E-\chi_{0,-i'}}\right) - t_0(E-\chi_{0,0})} + \frac{t_{i',2}^2}{t_0(E-\chi_{0,i'})} \quad (14)$$

In this notation $s_{11;\sigma\sigma'}$ and $s_{-1,-1;\sigma\sigma'}$ are the amplitudes of normal transmission of electron and hole channels, respectively, and $s_{1,-1;\sigma\sigma'}$, $s_{-1,1;\sigma\sigma'}$ the amplitudes of the Andreev reflection.

If M is odd, there is an unpaired electron on the grain before tunnelling. A tunnelling electron with spin opposite to this unpaired electron can be transmitted through the grain via a paired intermediate state. In this case there is a mixing for both the spin and pseudo-spin degrees of freedom. Thus there are four channels coupled, as shown in figure 1(b). In this case there is an intermediate state with $M + 1$ electrons on the grain shown by the close circle and several intermediate states with $M - 1$ and $M + 3$ electrons on the grain, denoted by the open circles in figure 1(b). The latter represent the cotunnelling process in which two electrons or two holes appear in the leads. The expressions for the transmission and reflection coefficients can be obtained from solving the corresponding Schrödinger equations

$$s_{ii';\sigma\sigma'}(M) = \frac{2ie^{i(k_i+k_{i'})}\sqrt{\sin(k_i)\sin(k_{i'})}u_{ii'}}{2e^{ik_{i'}}v_{ii'} - 1} \quad (15)$$

where

$$u_{ii'} = -\frac{t_{i,3}t_{i',3}\left(1 - \frac{2e^{ik_{i'}}t_{-i,4}^2\delta_{i,i'}\delta_{\sigma,-\sigma'}}{t_0(E-\chi_{1,-i})}\right)}{4e^{ik_{i'}}\left(t_{-i',3}^2 + t_{-i',4}^2\frac{E-\chi_{1,0}}{E-\chi_{1,-i'}}\right) - t_0(E-\chi_{1,0})} + \frac{t_{i,4}^2\delta_{i,i'}\delta_{\sigma,-\sigma'}}{t_0(E-\chi_{1,i})} \quad (16)$$

$$v_{ii'} = -\frac{2t_{i',3}^2\left(1 - \frac{2e^{ik_{i'}}t_{-i',4}^2}{t_0(E-\chi_{1,-i'})}\right)}{4e^{ik_{i'}}\left(t_{-i',3}^2 + t_{-i',4}^2\frac{E-\chi_{1,0}}{E-\chi_{1,-i'}}\right) - t_0(E-\chi_{1,0})} + \frac{2t_{i',4}^2}{t_0(E-\chi_{1,i'})} \quad (17)$$

with

$$\begin{aligned} t_{i,3(4)} &= \langle \psi_{i,3(4)} | H_C | \Phi(M - i + 1, S, -\sigma, -1, \sigma) \rangle \\ \psi_{i,3} &= \Phi(M + 1, 0, 0) \\ \psi_{i,4} &= \Phi(M - 2i + 1, 0, 0, -1, \sigma, \hat{i}, -\sigma) \end{aligned} \quad (18)$$

and

$$\chi_{1,0} = \mathcal{E}(M + 1, 0), \chi_{1,i} = \mathcal{E}(M - 2i + 1, 0) + 2 \text{sign}(i)\epsilon_0. \quad (19)$$

By applying a bias voltage V_b , there are two contributions to the current: the normal tunnelling and the Andreev reflection. The tunnelling current can be calculated from elements of the transmission matrix and the Landauer–Bütticker formula

$$I = \frac{e}{h} \int dE \sum_{M,i,i',\sigma,\sigma'} |s_{ii';\sigma\sigma'}(E, M)|^2 \left[F_i \left(E - \frac{ieV_b}{2}, M - i + 1 \right) \right. \\ \times F_{-i'} \left(E + \frac{i'eV_b}{2}, M - i' + 1 \right) - F_i \left(E + \frac{ieV_b}{2}, M - i + 1 \right) \\ \left. \times F_{-i'} \left(E - \frac{i'eV_b}{2}, M - i' + 1 \right) \right] \quad (20)$$

where $F_i(E, M)$ is the thermal distribution probability at energy E of many-body states with M electrons on the grain and an electron ($i = 1$) or a hole ($i = -1$) in the lead. We assume the local equilibrium for the grain and leads. Thus the statistical factor can be written as

$$F_1(E, M) = P(M, T) f(E - \mathcal{E}(M), T) \quad (21)$$

$$F_2(E, M) = P(M, T) [1 - f(E - \mathcal{E}(M), T)] \quad (22)$$

where $P(M, T)$ is the thermal probability of grain state $\Psi(M)$, and $f(E, T)$ is the Fermi distribution of electrons in the leads.

By taking the limit $V_b \rightarrow 0$, one can obtain the linear conductance

$$G = -\frac{e^2}{h} \int dE \sum_{M,i,i',\sigma,\sigma'} k_B T |s_{ii';\sigma\sigma'}(M)|^2 P_i(M - i + 1, T) \\ \times P_{i'}(M - i' + 1, T) \frac{\partial f(E - \mathcal{E}(M - i + 1), T)}{\partial E}. \quad (23)$$

The contribution from Andreev reflection is from the terms with $i \neq i'$, for which the statistical factor $F_i(E, M - i + 1, T)F_{i'}(E, M - i' + 1, T)$ becomes large at low temperature only when $\Psi(M)$ and $\Psi(M + 2)$ are nearly degenerate and have the lowest energy. Thus, the degeneracy of the grain ground state with a state having an extra pair can be regarded as a condition for observing the Andreev reflection. From equation (7) it can be seen that this condition can be satisfied at certain values of gate voltage only when $\Delta_M \equiv \mathcal{E}_0(M) - [\mathcal{E}_0(M + 1) + \mathcal{E}_0(M - 1)]/2$, the parity gap, is greater than the charging energy $\frac{e^2}{2C}$. On the other hand, the terms with $i = i'$ give the contribution from normal tunnelling, which reaches a maximum at resonances as in a normal quantum dot.

3. Numerical results of tunnelling conductance

From the above analysis it can be seen that there is a remarkable difference in the Andreev reflection between even and odd M . Before calculation of conductance one should specify the occupation status of the grain. By sweeping the gate voltage V_g , M can be sequentially changed. From inequality (7), the length of interval of V_g in which the particle number is M can be expressed as

$$\delta V_g(M) = \begin{cases} \frac{e^2}{C} - 2\Delta_M & \text{if } \frac{e^2}{C} > 2\Delta_M \\ 0 & \text{otherwise.} \end{cases} \quad (24)$$

For even M the interval $\delta V_g(M)$ is always finite because of the negative Δ_M due to the pairing. For odd M , Δ_M is positive. Thus, if $\Delta_M > \frac{e^2}{2C}$, M will be always even and changed by two each time in sweeping V_g . On the other hand, if the Coulomb energy is larger, $\Delta_M < \frac{e^2}{2C}$, M

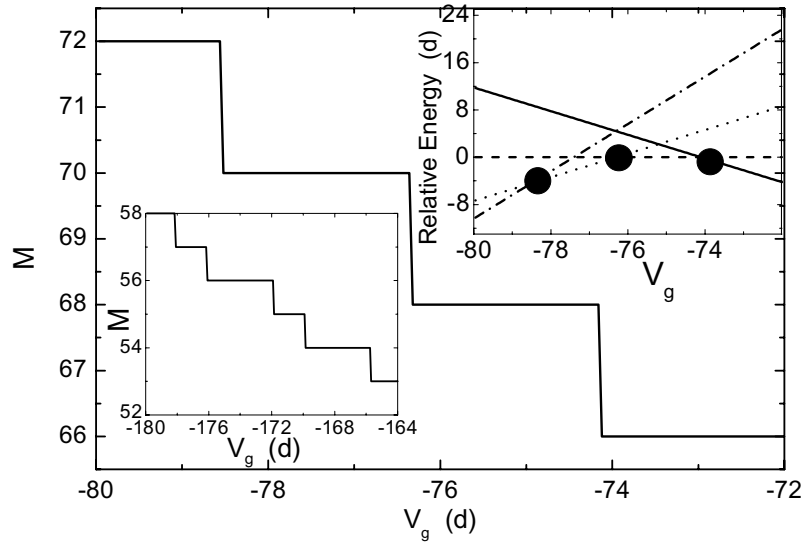


Figure 2. Grain particle number M as a function of the gate voltage V_g . The single-particle levels range as $\epsilon_j^0 = jd$, for $j = 1, 2, \dots, N$ with $N = 90$. The BCS pairing strength is $\lambda = 0.18$. The Coulomb energy is $e^2/(2C) = 0.3d$. The upper inset is the corresponding energy of state $\Psi(M)$ related to the energy of $\Psi(M = 68)$ for $M = 66$ (solid line), $M = 68$ (dashed line), $M = 70$ (dotted line) and $M = 72$ (dot-dashed line). The circles indicate the degeneracy of $\Psi(M)$ and $\Psi(M \pm 2)$. The lower inset displays M as a function of V_g for strong Coulomb interaction ($e^2/(2C) = 1.3d$) where odd occupations appear.

can be changed one by one but with different intervals for even and odd M . This situation is illustrated in figure 2, where M is plotted as a function of V_g and the corresponding energies for states with different M are shown. In the case of $\Delta_M > \frac{e^2}{2C}$ states $\Psi(M)$ and $\Psi(M + 2)$ are lowest lying and degenerate at values of V_g where M jumps by two. Thus, the contribution to the conductance from the Andreev reflection is expected to reach the maximum at these values of V_g . For $\Delta_M > \frac{e^2}{2C}$ M jumps between even and odd and at the jumping points $\Psi(M)$ is degenerate with $\Psi(M + 1)$ rather than $\Psi(M + 2)$. In this case the contribution from the Andreev reflection is small in the whole range of V_g . This implies that although the Coulomb blockade has no effect on the inner spectrum of the superconducting grain except for a constant shift, it does destroy the outer superconducting appearance, such as the Andreev reflection.

From the obtained occupation M and the corresponding energies we calculate the conductance for various parameters. In figure 3 we plot G in the case of weak Coulomb interaction ($\Delta_M > \frac{e^2}{2C}$) as a function of V_g for different temperatures. The main peaks appear at the gate voltages where states $\Psi(M)$ and $\Psi(M + 2)$ are degenerate, corresponding to the contribution from the Andreev reflection. The peaks are lowered and widened by increasing the temperature, implying the destruction effect of the thermal fluctuations. Between two main peaks a lower peak appears, corresponding to the contribution of the cotunnelling process represented by the broken lines and open circles in figure 1(a). In this case the occupation number on the grain is even, thus the cotunnelling does not change the spin and pseudo-spin indices, leaving the paired grain state unchanged after tunnelling. This is different from the cotunnelling of the normal quantum dots that changes the spin indices and leads to the Kondo effect in the valley regime. However, the temperature dependence of these lower peaks is similar to that

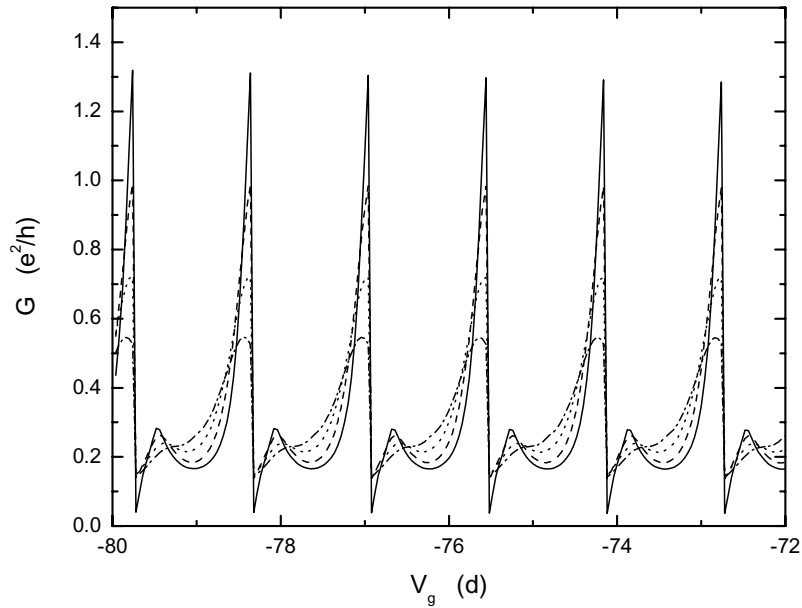


Figure 3. The conductance as a function of the gate voltage for different temperatures in the case of weak Coulomb interaction $e^2/(2C) = 0.1d$. The other parameters are the same as those in figure 2. $k_B T = 0.05d$ (solid line), $0.1d$ (dashed line), $0.15d$ (dotted line) and $0.2d$ (dash-dotted line).

of the cotunnelling in the normal dots. Since there are only even occupations, the peaks can be used to count the number of the pairs on the grain, rather than the single electrons.

In figure 4 we plot the conductance versus gate voltage in the case of intermediate Coulomb interaction $\frac{e^2}{2C} \sim \Delta_M$. The contribution from the normal tunnelling is increased. The main peaks correspond to the contribution from the Andreev reflection, while the lower peaks are from the resonances in the odd occupations. The latter is much weaker than the former because of the low thermal probability of the odd occupations. Note that in the shorter valleys between high and low peaks the conductance is lowered by increasing the temperature due to the cotunnelling process. In this case the cotunnelling can partly lead to a spin-flip like the Kondo effect in the normal quantum dot.

The behaviour of tunnelling conductance in the case of strong Coulomb interaction $\frac{e^2}{2C} > \Delta_M$ is displayed in figure 5. In this case the contribution from the normal tunnelling is dominant. The main peaks correspond to resonances in both odd and even occupations. There are two small shoulders beside a resonance peak of the odd occupation. They are due to the cotunnelling in particle and hole channels, respectively, which lead to the Kondo effect with spin-flip on the grain. The behaviour is similar to that of the normal quantum dots, except for the different peak spacing between the odd and even occupations, reminiscent of the remainder of the pairing gap, and the cotunnelling in two (particle and hole) channels.

In figures 6 and 7 we show P_A and P_S , the fractions of contributions from Andreev reflection and spin-flip cotunnelling to the conductance, respectively. From figure 6 it can be seen that the Andreev reflection occurs only in narrow ranges of V_g , reflecting the restriction on variation of particle number of the grain. The peak height is reduced by increasing the Coulomb interaction, and approaches zero in the case of strong interaction. In contrast, by increasing interaction the peak height of the spin-flip cotunnelling is increased from zero, as

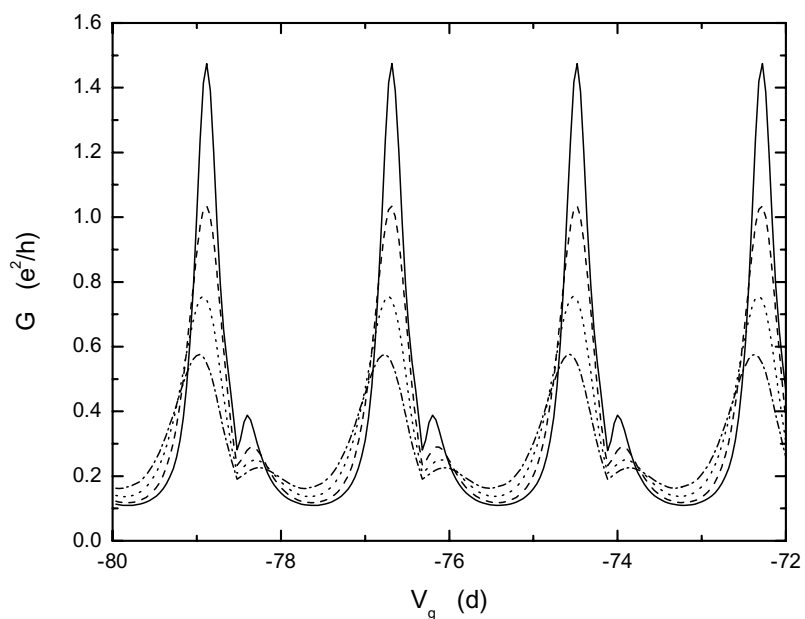


Figure 4. The same as in figure 3 but with $e^2/(2C) = 0.3d$.

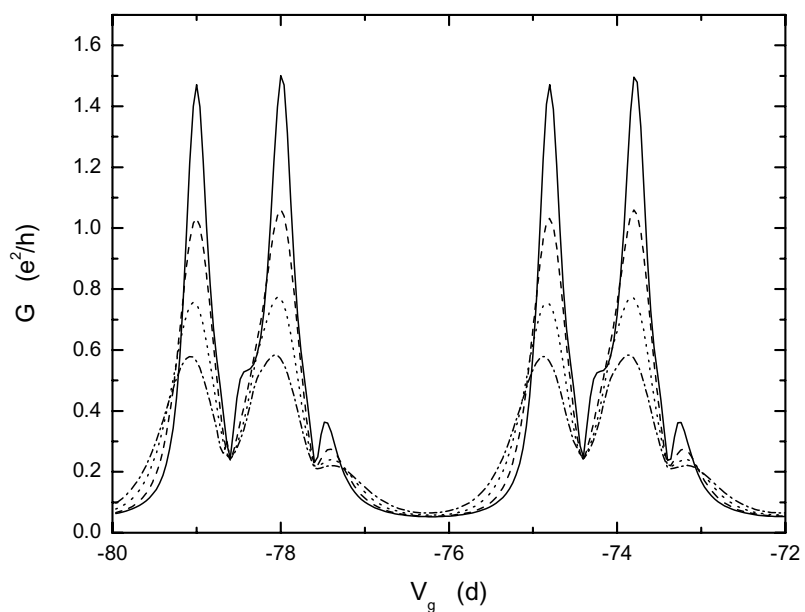


Figure 5. The same as in figure 3 but with $e^2/(2C) = 0.8d$.

can be seen from figure 7. There are two cotunnelling peaks corresponding to the shoulders beside a resonance peak of odd occupation in figure 5. They are produced by two intermediate states in particle and hole channels which have different energies and electron numbers on the grain. The peaks of P_S are narrow because only the low order of cotunnelling process in real space is included in the present calculation.

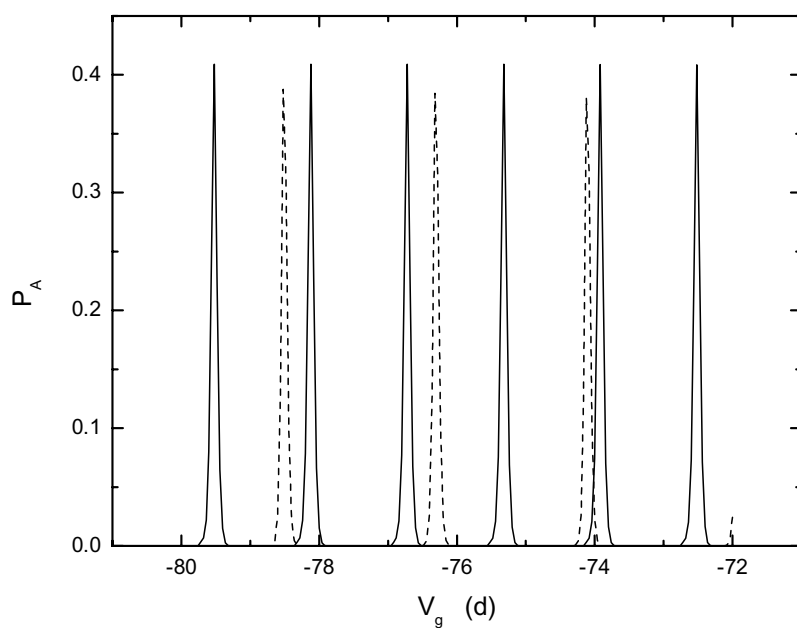


Figure 6. The fraction of contribution from Andreev reflection to the conductance P_A as a function of the gate voltage. $e^2/(2C) = 0.1d$ (solid line), $0.3d$ (dashed line) and $0.8d$ (dotted line). $k_B T = 0.05d$ and the other parameters are the same as those in figure 3. For $e^2/(2C) = 0.8d$ $P_A \sim 0$, so the dotted curve could not be seen.

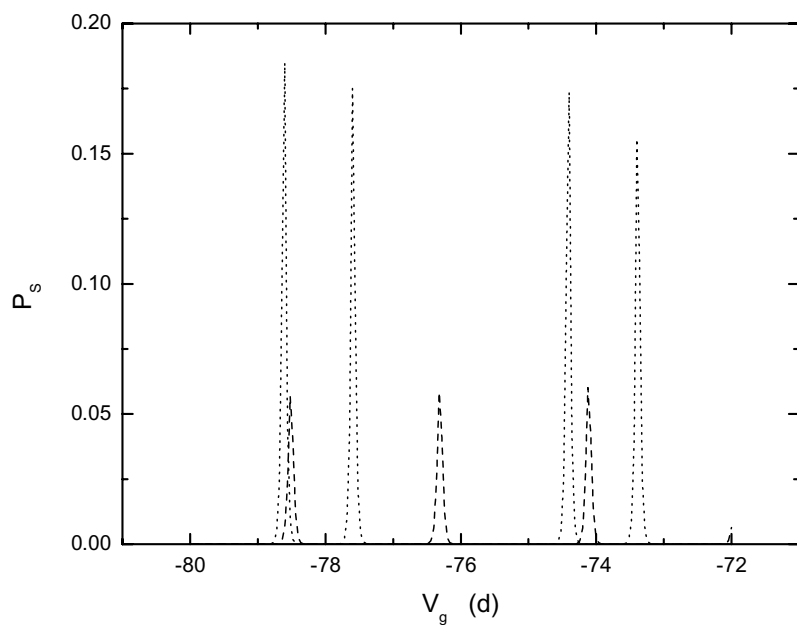


Figure 7. The fraction of contribution from spin-flip cotunnelling to the conductance P_S as a function of the gate voltage. The parameters are the same as those in figure 6. For $e^2/(2C) = 0.1d$ $P_S \sim 0$, so the solid curve cannot be seen.

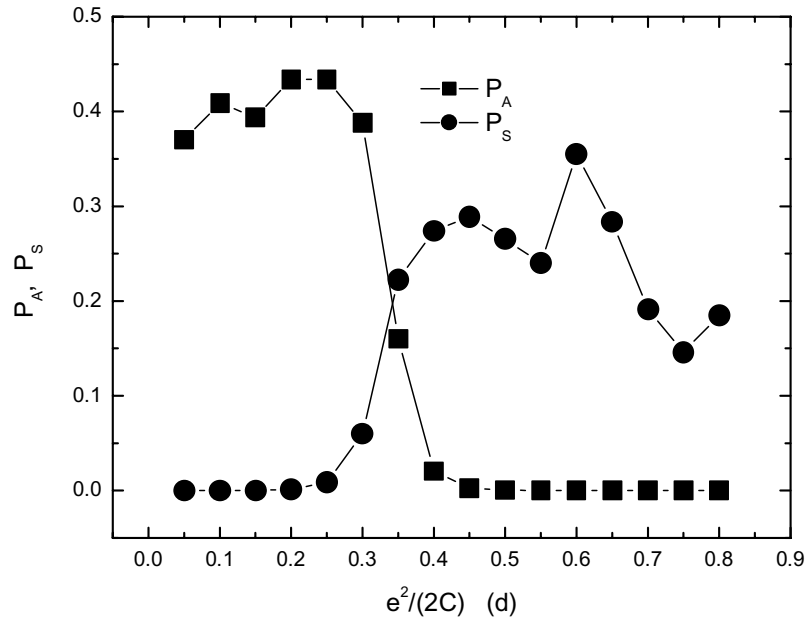


Figure 8. The peak intensities of P_A and P_S as functions of Coulomb interaction. The parameters are the same as those in figure 6.

Since the Andreev reflection is suppressed by the Coulomb interaction and the Kondo effect is suppressed by the pairing, one can expect a crossover from the Andreev to the Kondo regime by increasing the interaction. Such a crossover is clearly displayed in figure 8, where P_A and P_S are shown as functions of the interaction. It can be seen that the crossover occurs near $e^2/(2C) \sim \Delta_M$. For $e^2/(2C) \ll \Delta_M$ the Kondo-type spin-flip transmission is nearly zero ($P_S \sim 0$) and the amplitude of Andreev reflection (P_A) is finite, while for $e^2/(2C) \gg \Delta_M$ P_S is finite and $P_A \sim 0$.

In this system there are three characteristic energies, level spacing d , pairing energy Δ_M and Coulomb interaction $e^2/(2C)$. As illustrated above the crossover is mainly determined by the values of Δ_M and $e^2/(2C)$. The level spacing only influences the internal spectrum of the grain. Generally, by reducing the size of the grain $e^2/(2C)$ is increased and Δ_M is decreased. Thus, the crossover from Andreev to Kondo behaviour could be observed by changing the size of the grain.

4. Conclusions

We have studied the Andreev reflection and Kondo effect in tunnelling through a superconducting grain in the presence of Coulomb interaction. The Andreev reflection is suppressed by the Coulomb interaction on the grain due to the fixing trend of electron number, while the Kondo effect is suppressed by the pairing due to the reduction of probability of odd occupations. Thus, in such systems the main energy scales are the pairing energy Δ_M and the charging energy $e^2/(2C)$. When $e^2/(2C)$ is increased from zero, the tunnelling conductance exhibits the crossover from Andreev behaviour to Kondo behaviour near the point $e^2/(2C) \sim \Delta_M$. This crossover reflects the transition of the system from the superconducting grain to the normal quantum dot.

Acknowledgment

One of the authors (S-JX) gratefully acknowledges the kind hospitality of the Institute of Physics, Academia Sinica in Taiwan.

References

- [1] Lafarge P, Joyez P, Esteve D, Urbina C and Devoret M H 1993 *Phys. Rev. Lett.* **70** 994
Eiles T M, Martinis J M and Devoret M H 1993 *Phys. Rev. Lett.* **70** 1862
Joyez P, Lafarge P, Filipe A, Esteve D and Devoret M H 1994 *Phys. Rev. Lett.* **72** 2458
- [2] Ralph D C, Black C T and Tinkham M 1995 *Phys. Rev. Lett.* **74** 3241
Black C T, Ralph D C and Tinkham M 1996 *Phys. Rev. Lett.* **76** 688
- [3] Hekking F W J, Glazman L I, Matveev K A and Shekhter R I 1993 *Phys. Rev. Lett.* **70** 4138
Hekking F W J, Glazman L I and Schön G 1995 *Phys. Rev. B* **51** 15312
Zaikin A D 1994 *Physica B* **203** 255
- [4] Jankó B, Smith A and Ambegaokar V 1994 *Phys. Rev. B* **50** 1152
- [5] von Delft J, Zaikin A D, Golubev D S and Tichy W 1996 *Phys. Rev. Lett.* **77** 3189
Smith R A and Ambegaokar V 1996 *Phys. Rev. Lett.* **77** 4962
- [6] Matveev K A and Larkin A I 1997 *Phys. Rev. Lett.* **78** 3749
- [7] Berger S D and Halperin B I 1998 *Phys. Rev. B* **58** 5213
Mastellone A, Falci G and Fazio R 1998 *Phys. Rev. Lett.* **80** 4542
Braun F and von Delft J 1998 *Phys. Rev. Lett.* **81** 4712
Dukelsky J and Sierra G 1999 *Phys. Rev. Lett.* **83** 172
- [8] Richardson R W 1977 *J. Math. Phys.* **18** 1802
Sierra G, Dukelsky J, Dussel G G, von Delft J and Braun F *Preprint cond-mat/9909015*
- [9] Xiong S-J and Xiong Ye 1999 *Phys. Rev. Lett.* **83** 1407